Supplemental Fig. 1

A

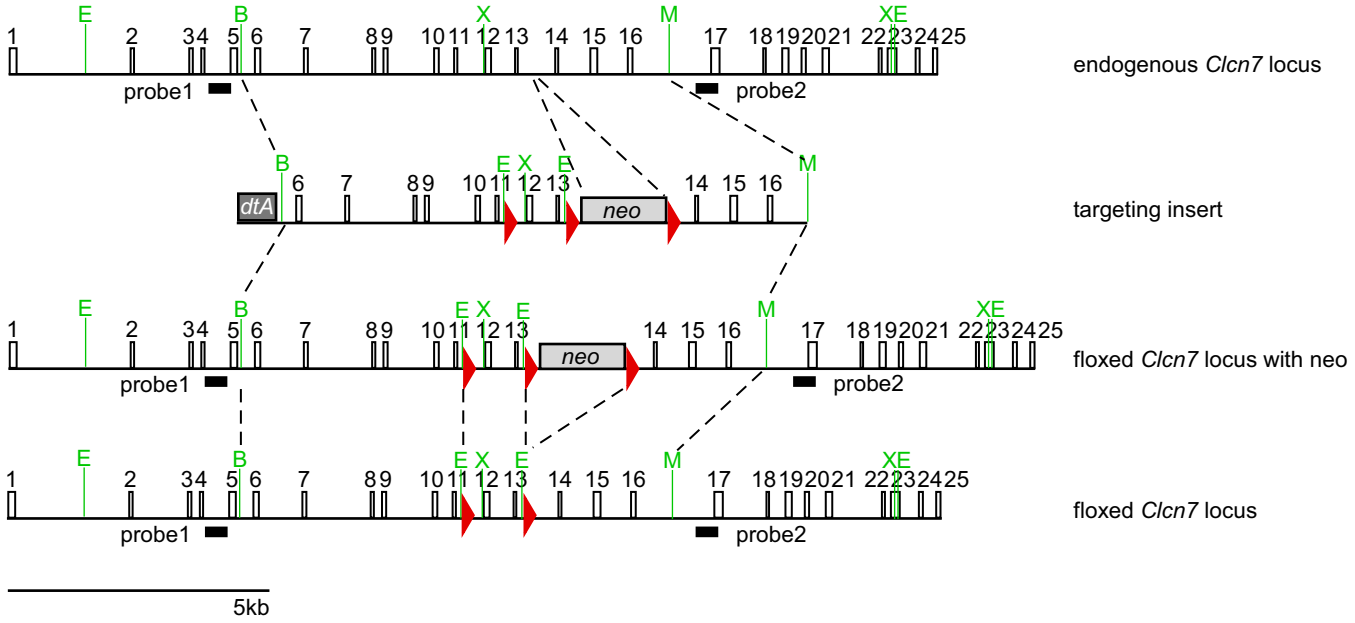

B

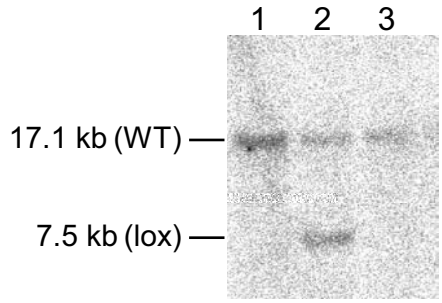

C

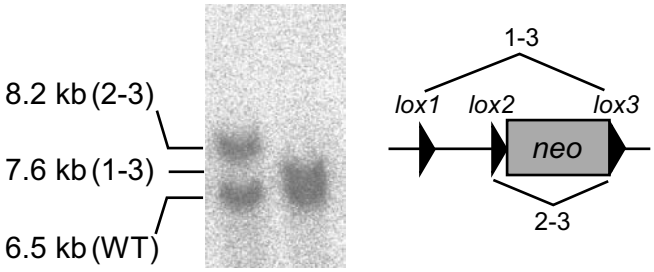

Supplemental Fig. 2

A

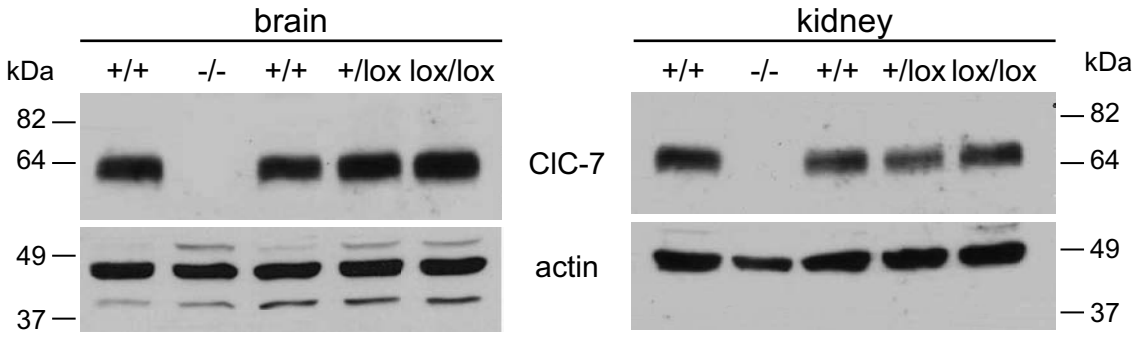

B

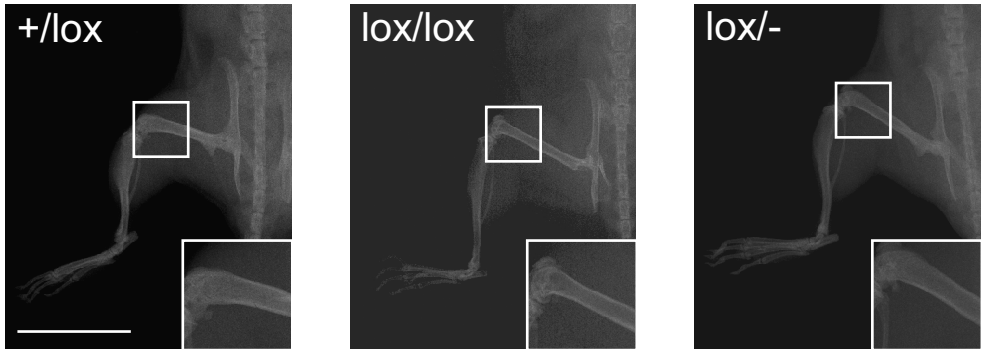

C

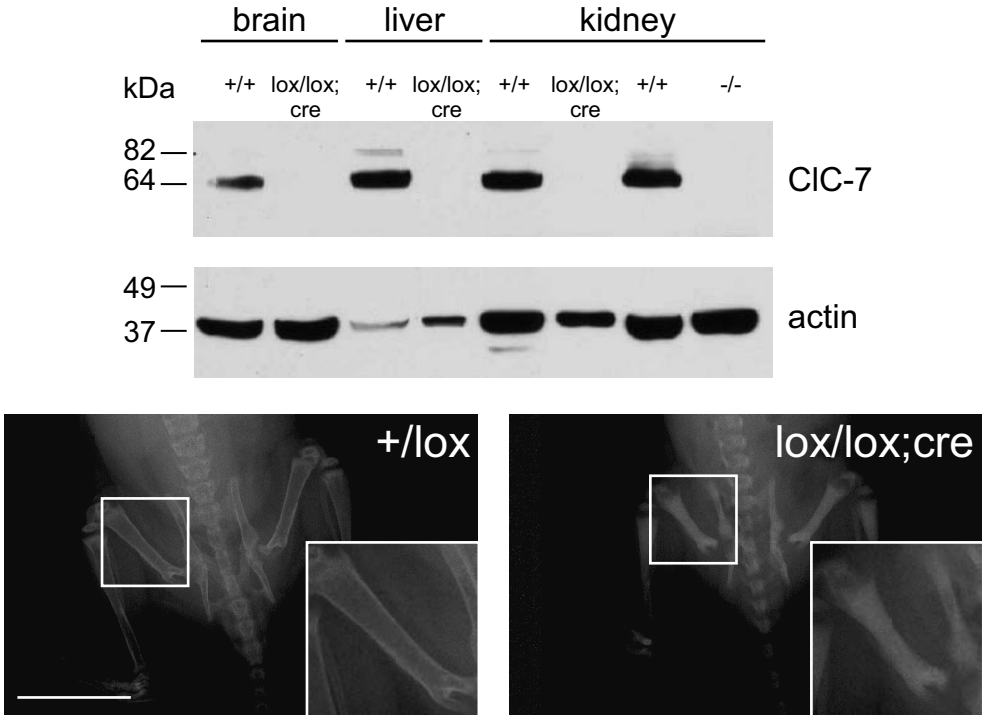

Supplemental Fig.3

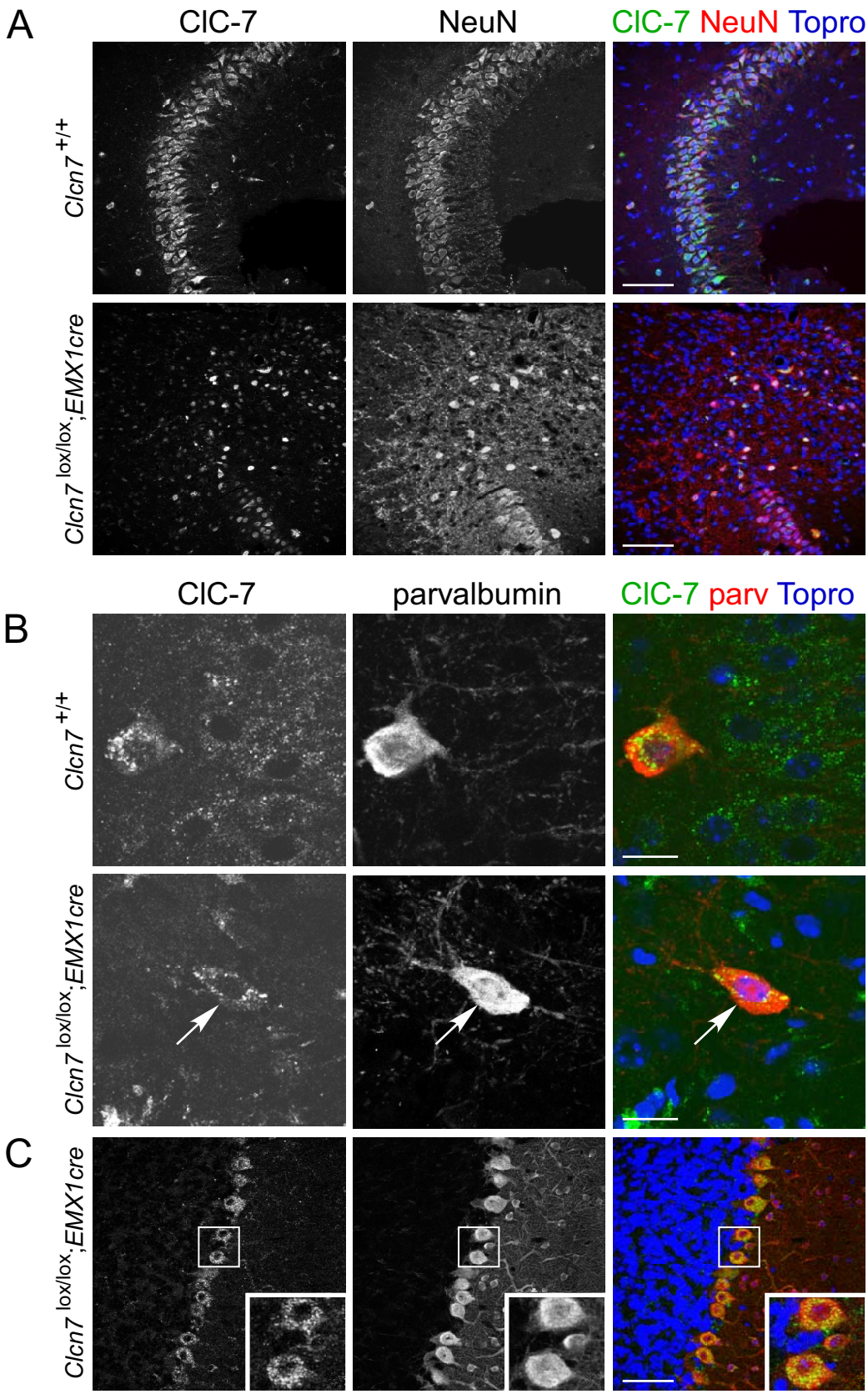

Supplemental Fig. 4

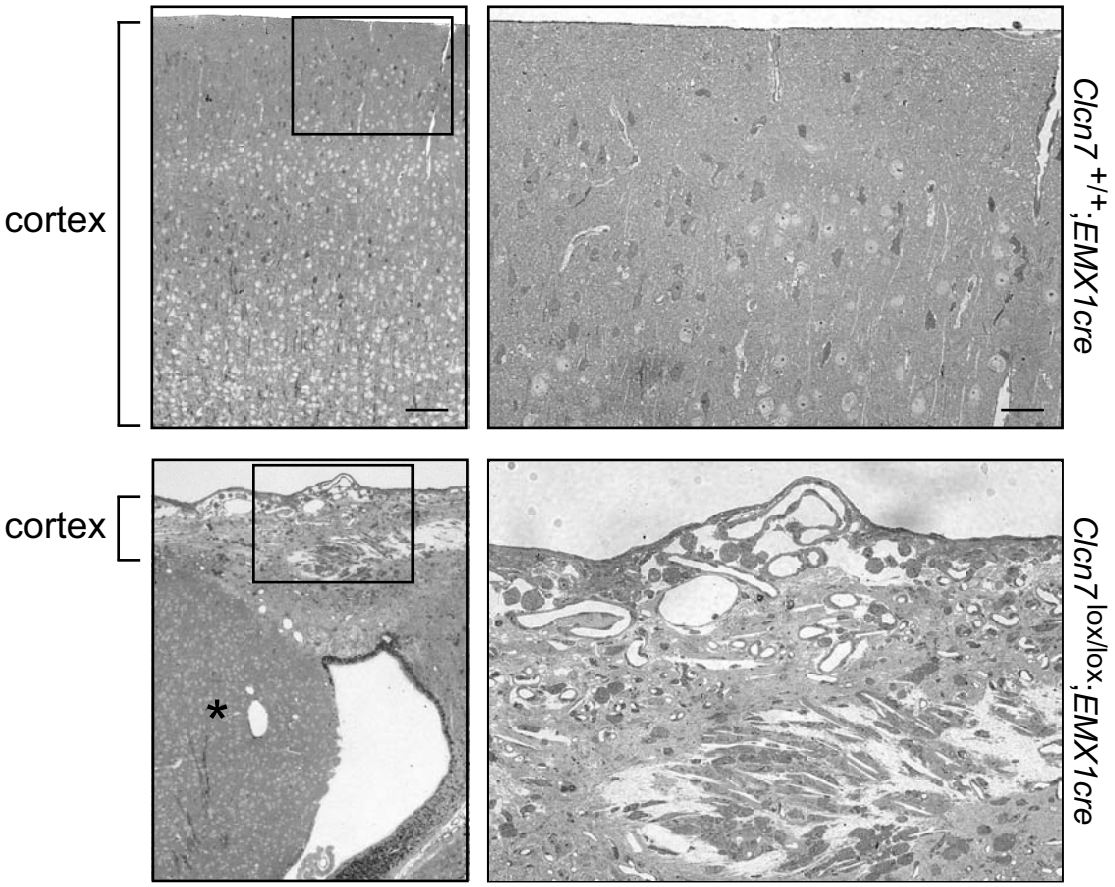

Supplemental Fig. 5

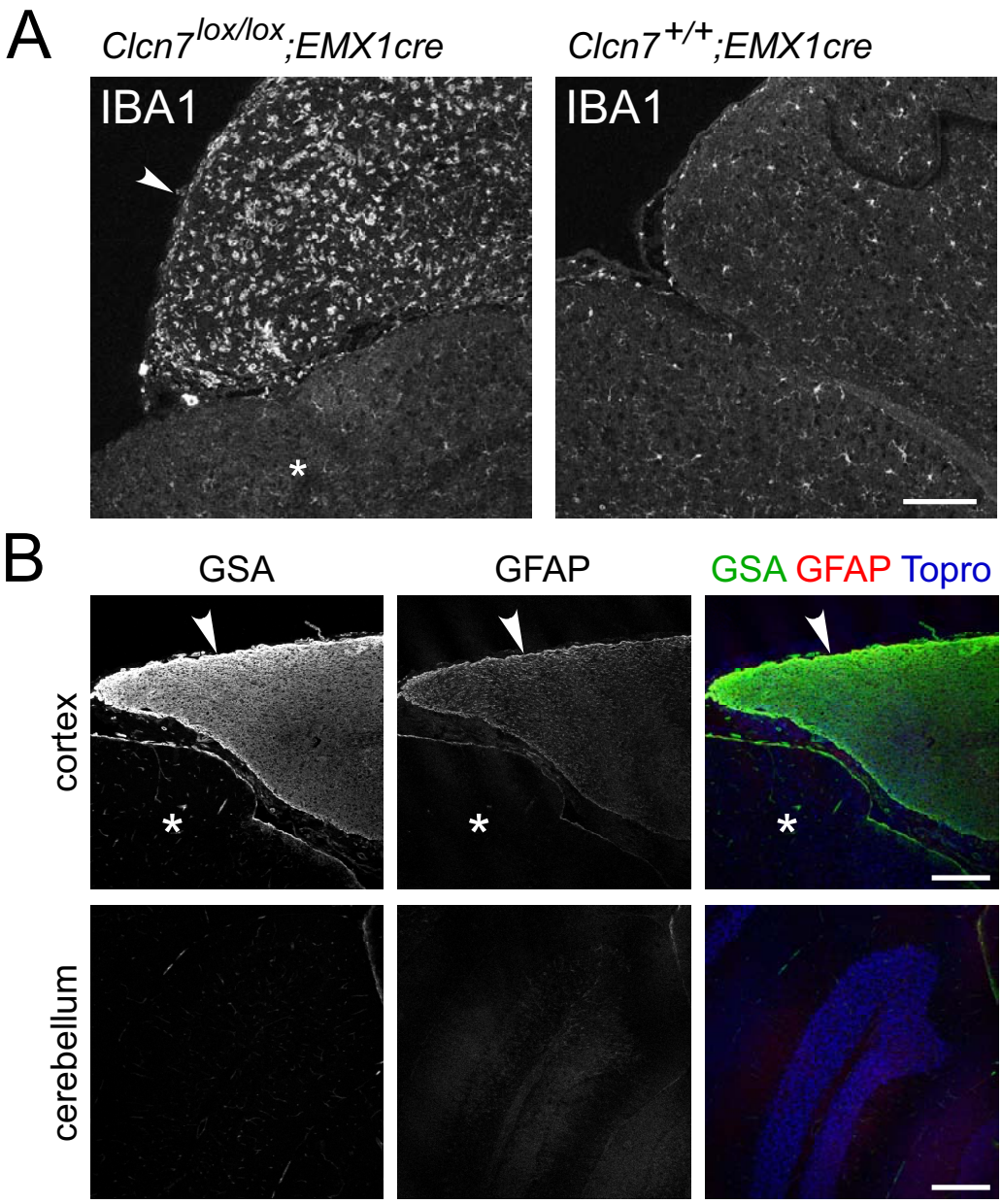

Supplemental Fig. 6

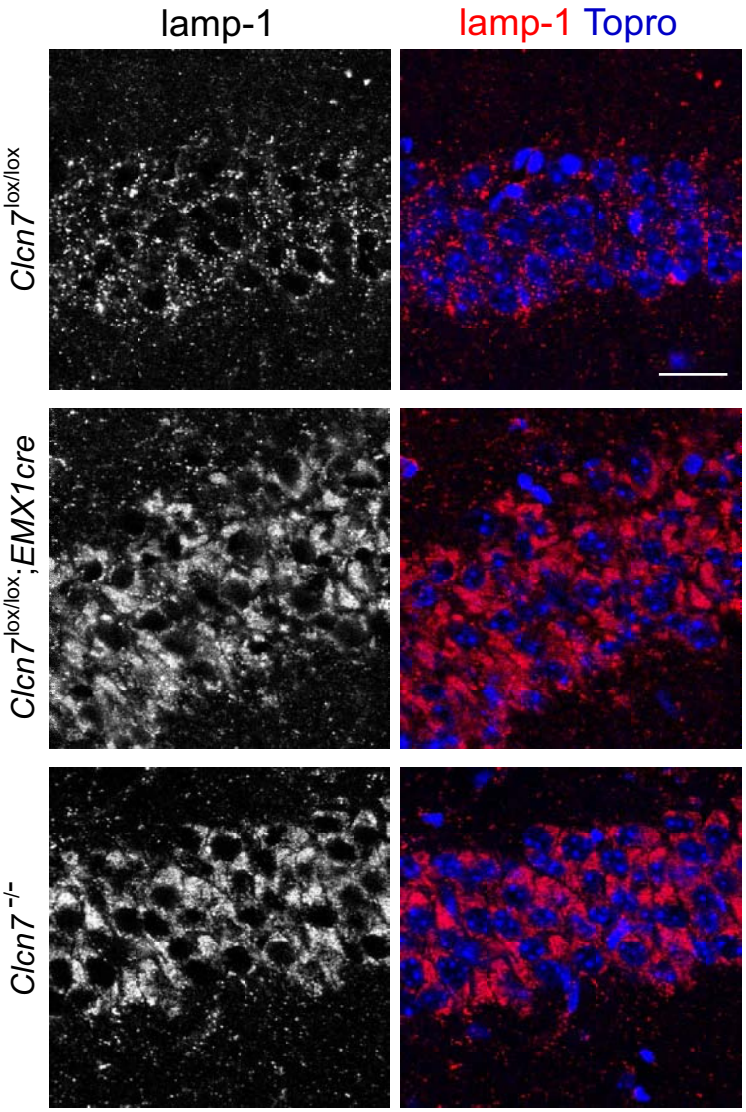

Supplemental Fig. 7

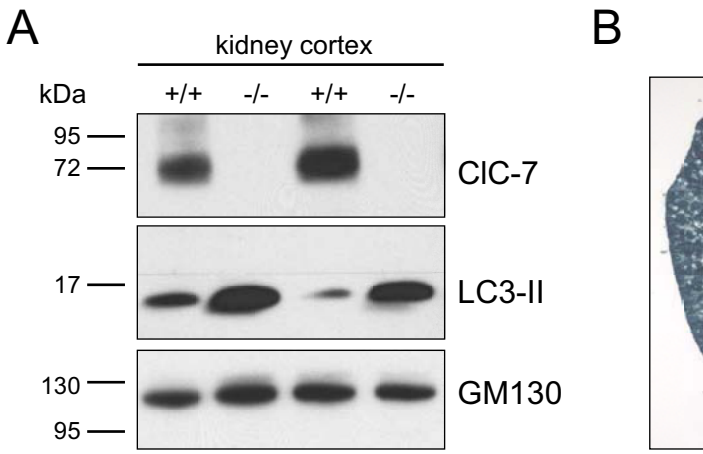

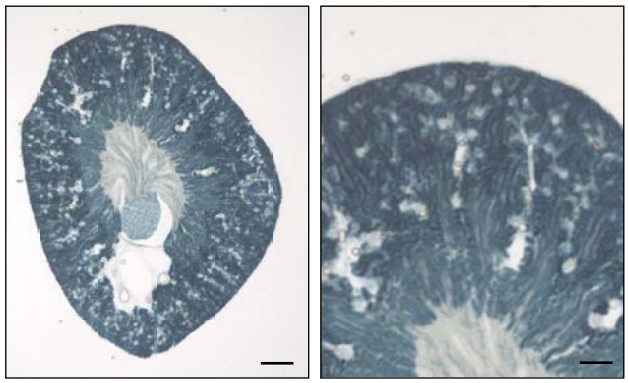

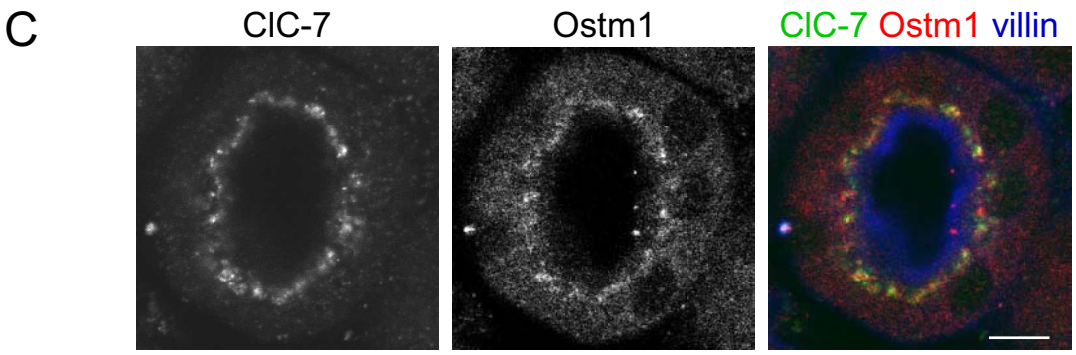

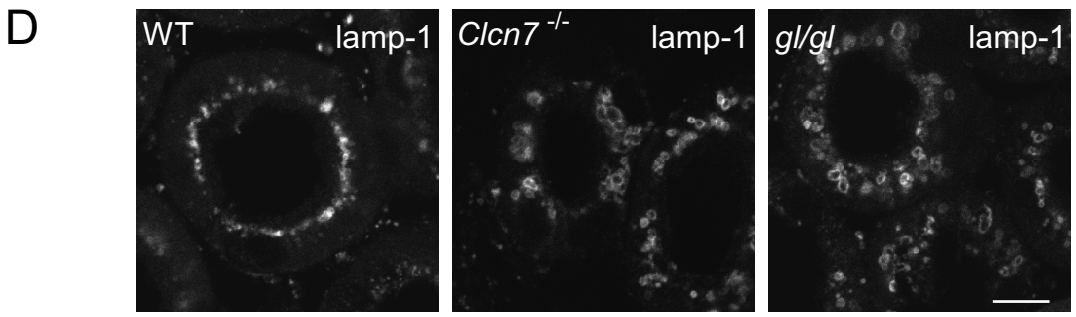

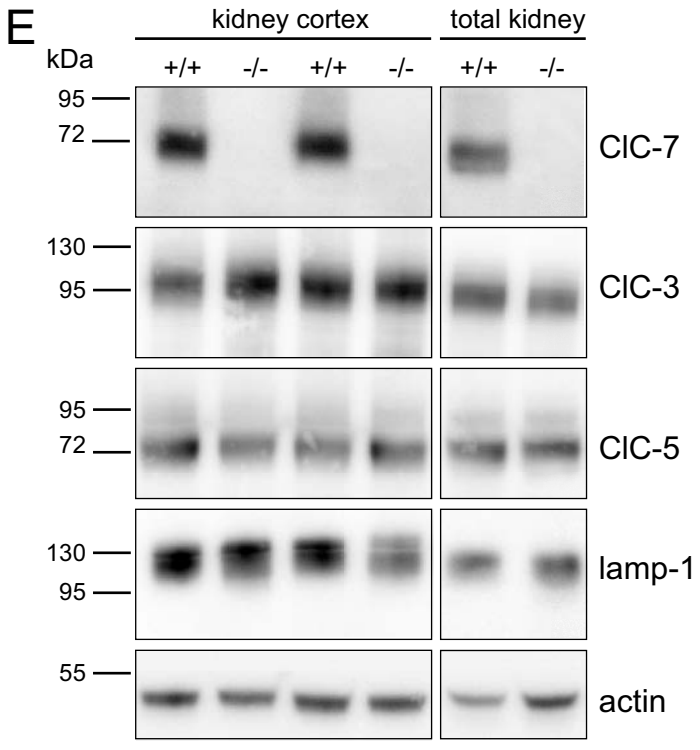

Supplemental Fig. 8

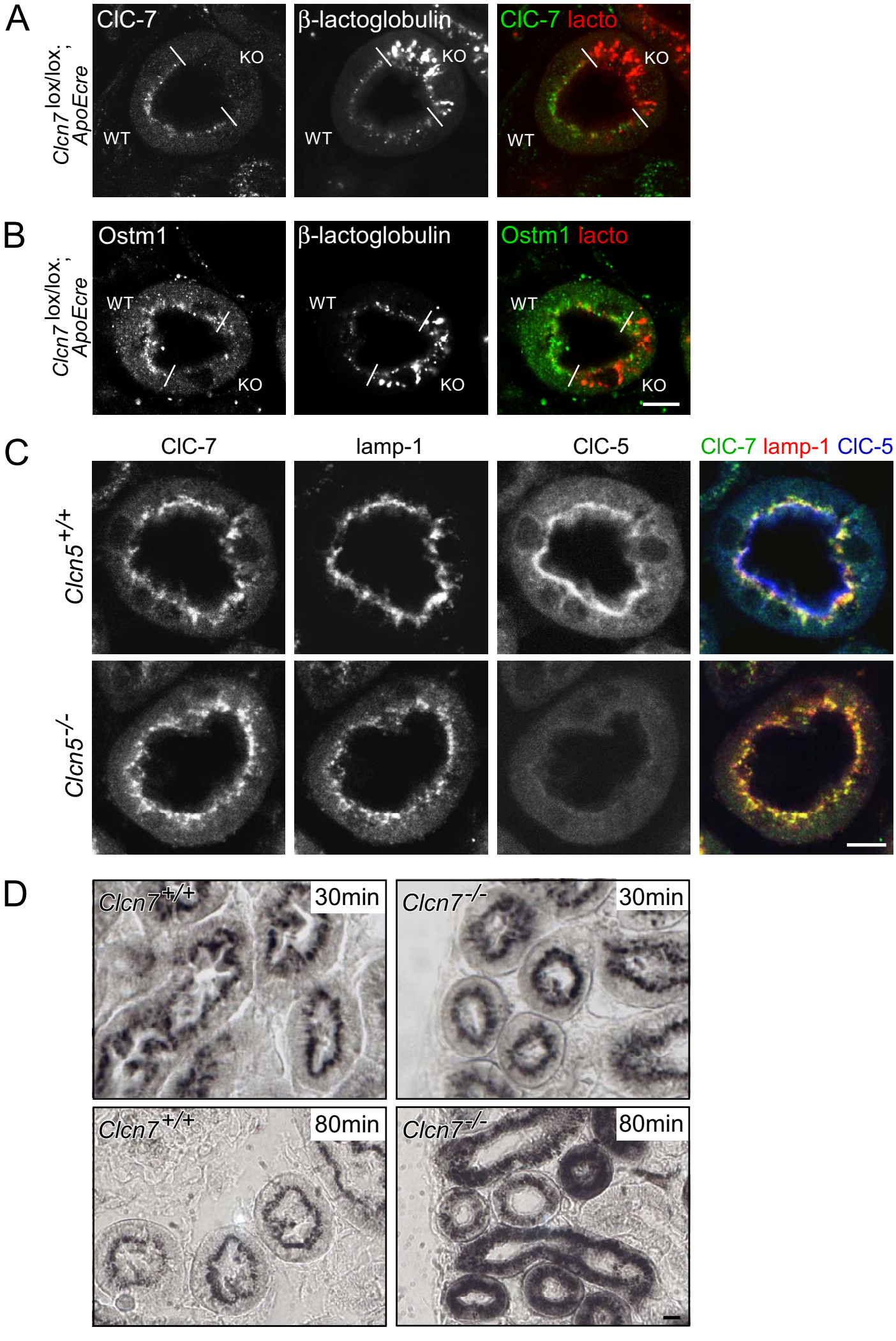

SUPPLEMENTAL INFORMATION

Supplemental Fig. 1. Generation of a 'floxed' ClC-7 mouse model. *A*) Targeting of the *Clcn7* gene. The top shows a genomic clone encompassing all exons of the *Clcn7* gene. The targeting vector and 'floxed' *Clcn7* locus after homologous recombination are depicted below (dtA: diphtheria toxin A cassette). The 'floxed' *Clcn7* locus was generated by removing the neomycin resistance (neo) cassette via cre-mediated recombination in embryonic stem (ES) cells. Important restriction sites (B=*Bsi*WI; E=*Eco*RI; M=*Mef*I; N=*Not*I; X=*Xmn*I), loxP-sites (red triangles) and probes used for Southern blot confirmation of recombination events are indicated. *B*) Southern blot and detection with probe 1 after EcoRI digest of ES cell DNA identified a homologous recombination event (WT: normal *Clcn7* locus; lox: floxed *Clcn7* locus). Lanes 1 and 3: WT clones, lane 2 heterozygous clone after integration of the targeting insert. *C*) After expression of cre recombinase in targeted ES cells, loss of the neo cassette was confirmed via Southern blot with probe 2 after digestion with *Xmn*I.

Supplemental Fig. 2. Immunoblot analysis and morphological studies of 'floxed' ClC-7 mice. *A*) Immunoblot analysis of brain (left) and kidney (right) lysates showed no alterations in ClC-7 protein levels in heterozygous (+/lox) or homozygous (lox/lox) 'floxed' *Clcn7* mice compared to WT littermates (+/+). No ClC-7 signal was present in ClC-7 KO mice (-/-). *B*) X-ray pictures revealed no changes in bone density of 'floxed' ClC-7 mice (lox/lox) or mice heterozygous for the 'floxed' and ClC-7 KO allele (lox/-) compared to control mice (+/lox). *C*) After crossing 'floxed' ClC-7 mice to *deleter*-cre mice, ClC-7 was absent from tissue lysates of offspring homozygous for the deleted 'floxed' *Clcn7* allele (lox/lox;cre) as shown by immunoblotting with an antibody directed against the amino-terminus of ClC-7. X-ray analysis revealed the typical osteopetrotic increase in bone mass in $Clcn7^{lox/lox}$*;cre* mice. Scale bars: 2.5 cm.

Supplemental Fig. 3. Deletion of ClC-7 in forebrain-specific KO mice. *A*-*C*) Brain sections of 38-days old mice were co-stained for ClC-7 and the neuronal marker NeuN (*A*) or parvalbumin, a marker for interneurons (*B*,*C*). A) In WT ($Clcn7^{+/+}$) mice, ClC-7

(green) was highly expressed in neurons of the hippocampal CA3 region. NeuN staining (red) revealed the loss of neurons in the hippocampal CA3 region of a forebrain-specific ClC-7 KO mouse (*Clcn7*$^{lox/lox}$*;EMX1cre*). No ClC-7-signal was detected in the majority of remaining hippocampal neurons. Apparent ClC-7 signal in KO mice is likely caused by autofluorescence of storage material (6). *B*) In the CA3 region, ClC-7 (green) was detected both in principal (pyramidal) cells, as well as in interneurons that were identified by parvalbumin-staining (red). In *Clcn7*$^{lox/lox}$*;EMX1cre* mice, ClC-7 was mainly expressed in parvalbumin-positive interneurons (arrow). *C*) As expected for the forebrain-specific KO, normal ClC-7 expression was observed in the cerebellum with strongest staining of Purkinje cells. Scale bars: 40 µm in *A*, and 20 µm in *B* and *C*.

Supplemental Fig. 4. Neurodegeneration in forebrain-specific ClC-7 KO mice. Semi-thin sections of the brain of 1-year old KO (*Clcn7*$^{lox/lox}$*;EMX1cre*) mice and controls (*Clcn7*$^{+/+}$*;EMX1cre*) were stained with toluidine blue. In KO mice, the cortex was massively degenerated and no neuronal structures could be identified. In the midbrain (asterisk) of those mice, where ClC-7 was not deleted, structures were normal and no neuronal loss was observed. Scale bars: 20 µm (left) and 5 µm (right).

Supplemental Fig. 5. Microgliosis and astrogliosis in the cortex of forebrain-specific ClC-7 KO mice. Brain sections were stained with an antibody against the microglia marker protein IBA1 (*A*) or with the microglia-binding lectin (GSA) and an antibody against the glial fibrillary acidic protein (GFAP, staining astrocytes) (*B*). *A*) Intense IBA1 staining of microglia was present in the cortex (arrowhead) of 46-days old *Clcn7*$^{lox/lox}$*;EMX1cre* mice but not in *Clcn7*$^{+/+}$*;EMX1cre* controls. (*B*) Microgliosis and astrogliosis in the cortex of 20-weeks old *Clcn7*$^{lox/lox}$*;EMX1cre* mice (arrowhead). Activated astrocytes and microglia were never observed in those brain regions of 20-weeks old *Clcn7*$^{lox/lox}$*;EMX1cre* mice where ClC-7 was not deleted, such as the midbrain (asterisk in *A* and *B*) or the cerebellum (*B*, lower panel). Scale bars: 300 µm.

Supplemental Fig. 6. Lysosomal storage phenotype in forebrain-specific ClC-7 KO mice. Antibody staining identified altered lamp-1 distribution in hippocampal CA1 neurons of *Clcn7*$^{lox/lox}$*;EMX1cre* mice and constitutive ClC-7 KO mice (*Clcn7*$^{-/-}$) at the age of 38 days. DNA was stained with Topro. Scale bar: 25 µm.

Supplemental Fig. 7. ClC-7/Ostm1 in the kidney. *A*) Immunoblot on membrane preparation of kidneys reveals a drastic increase in the autophagic marker protein LC3-II in global ClC-7 KO mice (-/-) compared to wildtype controls (+/+). *B*) X-Gal staining of kidney sections of mice expressing a ClC-7/lacZ fusion protein (blue). ClC-7 was detected in all regions of the kidney. *C*) ClC-7 co-localizes sub-apically with its β-subunit Ostm1 in PT cells of WT mice. Villin stains brush-borders and is a marker of PTs. *D*) Altered lamp-1 distribution in PT cells of ClC-7 KO (*Clcn7*$^{-/-}$) and Ostm1-deficient *grey lethal* (*gl/gl*) mice but not in controls (WT). *E*) Immunoblot on kidney cortex membrane preparations or total kidney lysates did not show any consistent alteration in the amount of endosomal or late endosomal/lysosomal membrane proteins between wildtype (+/+) and ClC-7 KO (-/-) mice, including the related vesicular CLC proteins ClC-3 and ClC-5. Scale bars: 50 µm (left) and 14 µm (right) in *B*, and 20 µm in *C* and *D*. (Age: 3-4 weeks).

Supplemental Fig. 8. Loss of ClC-7 disrupts the degradation of endocytosed protein in PT cells. *A,B*) Kidney-specific ClC-7 KO mice (*Clcn7*$^{lox/lox}$*;ApoEcre*) were injected intravenously with fluorescently labeled β-lactoglobulin. 1 h after injection, β-lactoglobulin fluorescence (red) was much more intense in ClC-7 KO than in WT cells. WT PT cells were identified by immunofluorescence staining for ClC-7 (green) (*A*) The β-subunit Ostm1 (green) was present in WT cells but undetectable in ClC-7 KO cells of chimeric tubules, identified by the stronger β-lactoglobulin fluorescence (*B*). *C*) Immunostaining on kidney sections shows normal expression and localization of ClC-7 and lamp-1 in PTs of ClC-5 KO mice (*Clcn5*$^{-/-}$). (*D*) 30 min after injection of the fluid-phase endocytosis substrate horseradish peroxidase (HRP), no major difference in HRP activity between WT (*Clcn7*$^{+/+}$) and global ClC-7 KO (*Clcn7*$^{-/-}$) was detected by direct 3,3'-diaminobenzidine (DAB) staining. After 80 min, a stronger HRP activity was observed in in PTs of *Clcn7*$^{-/-}$ compared to *Clcn7*$^{+/+}$ mice. Scale bars: 15 µm.